Ultrasonics Sonochemistry 83 (2022) 105924

Contents lists available at ScienceDirect

Ultrasonics Sonochemistry

journal homepage: www.elsevier.com/locate/ultson

Removal of field-collected Microcystis aeruginosa in pilot-scale by a jet pump cavitation reactor

Shuangjie Xu [a,b], Jiong Wang [a,b], Wei Chen [e], Bin Ji [a,c], Hengfei Yan [d], Zuti Zhang [a,b], Xinping Long [a,b,c,*]

[a] Hubei Key Laboratory of Waterjet Theory and New Technology, Hubei 430072, China
[b] School of Power and Mechanical Engineering, Wuhan University, Hubei 430072, China
[c] State Key Lab of Water Resources and Hydropower Engineering Science, Wuhan University, Hubei 430072, China
[d] Jiujiang Branch of Tianjin Navigation Instrument Research Institute, Jiangxi 32007, China
[e] State Key Laboratory of Freshwater Ecology and Biotechnology, Institute of Hydrobiology, Chinese Academy of Sciences, Wuhan University, Hubei 430072, China

ARTICLE INFO

Keywords:
Water treatment
Algal reduction
Microcystis aeruginosa
Hydrodynamic cavitation
Jet pump cavitation reactor
Cell disruption

ABSTRACT

Hydrodynamic cavitation has been investigated extensively in the field of water treatment in the last decade and a well-designed hydrodynamic cavitation reactor is critical to the efficient removal of algal and large-scale application. In this paper, a jet pump cavitation reactor (JPCR) is developed for the removal of cyanobacteria *Microcystis aeruginos* in a pilot scale. The results demonstrate that the photosynthetic activity of *M. aeruginosa* is greatly inhibited immediately after treatment in the JPCR, and the growth is also hindered after 3 days culture. Moreover, a high cell disruptions of *M. aeruginosa* is detected after treated by JPCR. The release of chlorophyll-a indicates that the JPCR caused serious rupture to *M. aeruginosa* cells. The plausible cell disruption mechanisms are proposed in accordance with a fluorescence microscope and scanning electron microscope. Then, the optimization of cell disruption efficiency is also investigated for various operating conditions. The results showed that the algal cell disruption efficiency is improved at higher inlet pressure and the cavitation stage between the unstable limited operation cavitation stage and stable limited operation cavitation stage. The effect and optimization of JPCR on algal reduction are highlighted. The results of the study promote the application of hydrodynamic cavitation on algal removal and provide strong support for JPCR application in algal removal.

1. Introduction

The seasonal explosive growth of cyanobacteria (also known as algal blooms) is among the most threatening environmental problem caused by the eutrophication of water bodies in the field of water treatment [1]. The reported eutrophic lakes have greatly increased in China during the past 30 years [2]. The seasonal explosive growth of cyanobacteria such as *M. aeruginosa* usually leads to serious problems such as oxygen depletion, phycotoxin production and high water turbidity [1]. These problems inhibit the growth of fish, aquatic plants and aquatic microfauna and greatly damage the ecosystem in water bodies [3]. Moreover, the hepatotoxin and microcystin generated during the metabolism of *M. aeruginosa* can contaminate surface water and threaten the health of humans and animals [4,5]. In developing countries, algal blooms are still a threat to human health and microalgae must be removed from water bodies immediately to ensure drinking water supplies.

Various methods and techniques have been developed to decrease the abundance of cyanobacteria. The eutrophication is mainly caused by the diffuse water pollution from agriculture and nutrient removal is the most effective method for algal removal which can warrant a positive long-term effect on the reduction of eutrophication in the polluted water body [6], thus reducing the abundance of algal blooms. But significant restriction of nutrient input to the surface water is almost impossible and unavailable for most areas across the world due to contemporary economical limitations nowadays.

Chemical treatment is the most common and cheapest method for algal removal because their effects on cyanobacteria are usually fast and effective (at least for a short period) [7]. However, the chemical treatment often suffers from residual heavy metal ions, associated harmful halides, changes in the pH of the water column, and difficulties in removing algal toxins, which can easily lead to secondary pollution [8,9]. The biological and ecological treatments seem to be effective in

* Corresponding author at: Hubei Key Laboratory of Waterjet Theory and New Technology, Hubei 430072, China.
E-mail address: xplong@whu.edu.cn (X. Long).

https://doi.org/10.1016/j.ultsonch.2022.105924
Received 12 December 2021; Received in revised form 9 January 2022; Accepted 16 January 2022
Available online 19 January 2022

controlling algae, but the control effect of algae blooms cannot be guaranteed in the case of poor water quality.

The mechanical treatment with the advantage of low cost and quick effect has aroused great interest. Clay coagulation is the most common method, but a high dose of coagulant is required for the algal removal in lakes [10], and microalgae are aggregated by clay adsorption and eventually settle to the bottom under the action of gravity. This method can only temporarily remove the algal cells from the water surface, but could not kill the algal cells completely. Moreover, the algal toxin could hardly be removed by this method.

Cavitation is considered a highly effective and sustainable mechanical approach to the removal of algae from the water system [11]. Cavitation can be defined as the formation, growth and collapse of bubbles in fluids when the local pressure is decreased to the saturated pressure [12]. The potential energy released during cavitation bubbles collapse could be used for algal removal [13]. The cavitation bubbles collapse induces extremely high temperatures (10000 K), high-pressure pulse (1000 atm), microjet and shear force [14,15], which would greatly damage cell structures and cellular organs. Highly reactive hydroxyl radicals (•OH) [16,17] generated from the homolytic cleavage of H_2O molecules could oxidize important constituents of microalgae and remove algal toxin released from the ruptured algal cells. Hydrodynamic cavitation has been successfully implemented in various applications with the main concern of environmental protection, such as the stabilization and safe reuse of sewage sludge [18–21]. Therefore, hydrodynamic cavitation, with the highly reactive hydroxyl radical's generation, may be also implemented for the algal removal in polluted water [22]. The cavitation can be easily induced by the ultrasonic wave and this type of cavitation is referred to as acoustic cavitation (AC). Satisfactory algal reduction could be achieved by using AC [13,22,23] and AC appears to be an efficient method for algal removal [24]. However, due to the rapid attenuation of ultrasound, only small volumes of algal suspensions can be treated. Therefore, AC is not suitable for large-scale algal removal with the disadvantage of high cost [25]. Hydrodynamic cavitation (HC) is caused by pressure variations in the flowing liquid due to a change in the geometry of the flowing system and it widely exists in hydraulic machineries such as Venturi tube [26], orifice plate [27], hydrofoils [28] and jet pump [29], in which numerous cavitation bubbles is easily induced. HC is usually considered harmful to hydraulic machinery due to the released energy by bubbles collapse, which can lead to material erosion, poor performance, limited life expectancies, noise and vibration [30–32]. But the released energy could be effectively utilized for algal removal in a well-designed hydrodynamic cavitation reactor with the advantage of high efficiency and large-scale operation [25]. Therefore, HC is an economical technique for algae removal and water treatment that can be used in large-scale operation with better energy efficiency than acoustic cavitation [33].

Cavitation intensity is the key influencing factor for the application of HC. Higher cavitation intensity results in more cavitation bubbles and higher cavitation collapse intensity which increase the cavitation effects (hot spot, microjet, etc) and the interaction between microorganism and cavitation bubbles. A well-designed cavitation reactor and the modeling of cavitation process to enhance cavitation effect are critical to promoting the algal reduction [34]. Venturi tubes and multi-orifice plates are common hydrodynamic cavitation reactors that are widely utilized in industrial applications. The cavitation occurring in multi-orifice plates reactor is mainly caused by shear flow due to the large velocity gradient [27,35] while cavitation in Venturi reactor is mainly induced by a sharp increase of velocity due to the reduction of flow channel area [36,37], which can lead to the reduction of local pressure to critical pressure. Jet pumps, also known as ejector pumps or ejectors, are traditional hydraulic machinery for heat and mass transfer through turbulent mixing [38]. The jet pump has no moving parts and thus has the advantages of reliable operation, easy processing, easy maintenance, and low cost [39]. Jet pumps are widely used in hydraulic engineering, energy engineering, mineral engineering and aerospace engineering [40–42]. However, jet pumps are prone to cavitation, resulting in degraded performance and unexpected noise and vibration. Conversely, jet pumps can serve as potential cavitation reactors when the objective is reversed (jet pump cavitation reactor, JPCR). A JPCR has intensive shear flow between the driving flow and suction flow, and low local pressure is also induced by the cross-section decrease of suction chamber, so cavitation generation in a JPCR is a combination of cavitation in Venturi cavitation reactors and orifice plate cavitation reactors. Developed cavitation with sufficient cavitation intensity could be achieved in a JPCR [43]. Therefore, JPCRs are of more potential as a cavitation reactor for algal removal with high cavitation intensity. Though the previous researches have shown the great potential of JPCRs for the algal removal [29,43–46], the applications of JPCR on the water treatment such as algal removal and corresponding mechanism are still partially understood.

In this paper, a jet pump cavitation reactor (JPCR) is proposed for algal removal with the advantage of high cavitation intensity, in which cavitation generation is a combination of cavitation in Venturi cavitation reactors and orifice plate cavitation reactors [29,43]. Jet pump cavitation reactors (JPCRs) are potential cavitation reactors for algal removal in which high cavitation intensity is generated. To this end, the JPCR is used alone to investigate the removal of *M. aeruginosa* in a pilot scale. The inhibitory effects of JPCR on the photosynthetic activity and growth of field-collected *M. aeruginosa* are evaluated. Moreover, the cell disruption efficiencies of JPCR are investigated based on the variation of chlorophyll-*a* concentration. Then the possible cell disruption mechanisms are proposed in accordance with a fluorescence microscope and scanning electron microscope. Finally, the optimization of flow parameters on cell disruption efficiency is also conducted.

2. Materials and methods

2.1. Cultivation of algae

The species used in the present study for the removal of microalgae is *M. aeruginosa*, collected directly from the field in Aquatic Seed Base, Institute of Aquatic Biology, Chinese Academy of Sciences. The pH of cell suspensions was around 8.2–8.6 and the temperature was kept stable at around 25 °C before experiments. The cell concentration was quantified by absorbance at wavelength 680 nm because 680 nm is the maximal absorbance band of *M. aeruginosa* cell suspensions. The absorbance of *M. aeruginosa* cell suspensions at wavelength 680 nm (optical density, OD_{680}) was measured by spectrophotometer (UV-722 N, Shanghai Science Instrument Company Limited, China). The concentration of collected cell suspensions was diluted to an algal bloom concentration of approximately 3×10^9 cells/L, corresponding to $OD_{680} = 0.25$. After dilution, a suspension of algae(35L) was introduced into JPCR and treated by hydrodynamic cavitation.

2.2. Experimental setup

The schematic diagram of JPCR and corresponding geometrical parameters is shown in Fig. 1. A JPCR consists of an inlet pipe, nozzle, suction chamber, suction pipe, throat and diffuser. The nozzle outlet diameter is 8 mm and the throat inlet diameter is 16 mm, so the area ratio (defined as the ratio of throat inlet area to nozzle outlet ratio) of JPCR in the present study is 4.00. A high-pressure driving flow is pumped into JPCR through the inlet pipe, then the high-speed driving flow is formed at the nozzle exit owing to the contractile structure of the nozzle. A low-speed suction flow is entrained into the suction chamber through the suction pipe due to the entrainment effect of high-speed jet flow. The driving flow and suction flow mix intensively in the throat, and the high-pressure pulsation caused by the velocity gradient between the two flows leads to intense cavitation in the shear layer. Owing to the contractile structure of the suction chamber, low local pressure also can be achieved in the jet pump cavitation reactor, which results in more

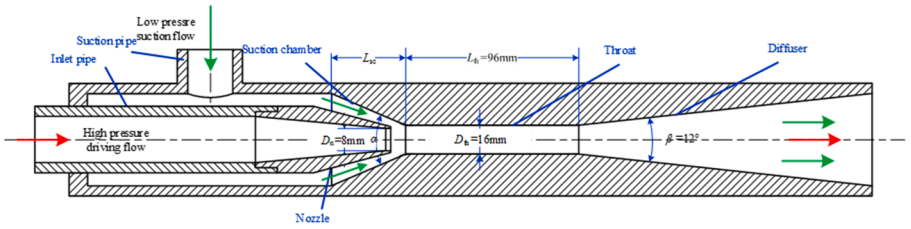

Fig. 1. The schematic diagram of JPCR.

intense cavitation than the traditional cavitation reactors. The intense cavitation collapses violently in the diffuser where the pressure gradually recovers.

In JPCR, the fundamental performance can be characterized by the variation of the pressure ratio, h, as a function of the flow ratio, q, (h-q curve). All the corresponding parameters can be defined as follow:

$$q = \frac{Q_s}{Q_{in}} = \frac{Q_{out}}{Q_{in}} - 1 \tag{1}$$

$$h = \frac{P_{out} - P_s}{P_{in} - P_s} = \frac{\left(\frac{p_{out}}{\rho g} + \frac{v_{out}^2}{2g} + z_{out}\right) - \left(\frac{p_s}{\rho g} + \frac{v_s^2}{2g} + z_s\right)}{\left(\frac{p_{in}}{\rho g} + \frac{v_{in}^2}{2g} + z_{in}\right) - \left(\frac{p_s}{\rho g} + \frac{v_s^2}{2g} + z_s\right)} \tag{2}$$

where Q is the flow rate, P is the total pressure, p is the absolute pressure, z is the elevation, v is the average flow velocity, subscripts th, n, in, s, out represent the throat inlet, nozzle exit, driving flow, suction flow, outlet flow respectively.

A schematic diagram of the experiment setup is shown in Fig. 2. This experimental setup is a closed loop that includes a water tank, a cooling water tank, a centrifugal pump, multiple ball valves, pressure sensors, electromagnetic flowmeter and JPCR. 35L suspensions of microalgae were contained in the water tank. The centrifugal pump with 11 kW power pumped the high-pressure cells suspension into JPCR. The temperature was stabilized at about 35 °C during the treatment by using the cooling water tank. The inlet pressure and outlet pressure can be regulated by ball valves installed at the inlet pipe and outlet pipe. The flow rate of driving flow and mixed flow also can be adjusted by valves and measured by electromagnetic flowmeters (KROHNE IFS400). Three pressure sensors (CHAOYU CY3011BCP70N) installed at the inlet, suction and outlet pipe were used to measure the absolute pressure. Pressure and flow data were recorded synchronously on a PC via PXI 6143 acquisition card.

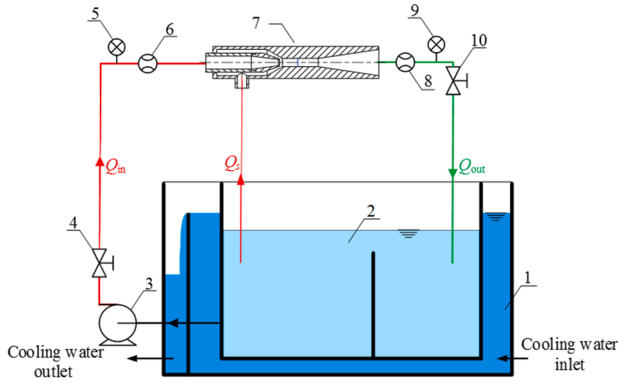

1-cooling water tank; 2-water tank; 3-centrifugal pump; 4,10-valves; 5,9-pressure sensor; 6,8-electromagnetic flowmeter; 7-JPCR.

Fig. 2. A schematic diagram of the experiment setup.

2.3. Analytical methods

Before starting, the control samples were taken. Samples of 250 mL were taken periodically after initiating the experimental setup. The inhibition effect on the photosynthesis and growth of *M. aeruginosa*, cell disruption efficiency of *M. aeruginosa* were quantified by testing all the samples after cavitation treatment. All the samples were tested three times and the standard deviations for the tested value are normally < 12%.

The photosynthetic activity of *M. aeruginosa* can be measured via a PHOTO-PAM (Heinz Walz, Effeltrich, Germany). Before testing, the samples were dark-adapted in a dark box for 30 min. Minimum (F_o) and maximum (F_m) fluorescence yields representing open and closed PSII reaction centers were determined, respectively. The widely used fluorescence parameter maximum PSII quantum yield Y, which can be defined as F_v/F_m=(F_m-F_o)/F_m, can be used to measure the maximum photochemical efficiency and indicate photosynthetic activity of PSII. The maximal relative electron transport rates through PSII (ETR_{max}) were also obtained by PHOTO-PAM.

The inhibition effect on the growth of *M. aeruginosa* could be quantified by the absorbance at wavelength 680 mm. The variations of optical density (OD_{680}) are strongly related to the concentration of the cell suspensions, which can quantitatively measure the growth of *M. aeruginosa*. Especially, to study the effect of hydrodynamic cavitation on the growth of *M. aeruginosa,* the treated cell suspensions were grown continuously in the incubator for 3 days and the optical density was monitored over this period. During cultivation, an illumination level of about 1000 lx was provided, and a light–dark cycle of 12 h:12 h was maintained.

The cell disruption efficiency can be quantified based on the chlorophyll-*a* concentration of the algal suspension immediately after cavitation treatment. The more algal cells were destroyed after treatment, the lower the chlorophyll-*a* concentration could be tested in extracted algal samples because the chlorophyll-*a* is released into the water after cell disruption. The taken samples were filtered through GF/C glass microfiber filter papers (diameter 47 mm) under a low vacuum. Chlorophyll-*a* was then extracted from the filter paper with 10 mL of 90% acetone. Acetone was placed in a refrigerator at 4 °C for 12 h after shaking. The 10 mL acetone was centrifuged (Jouan BR 4i, France) at 3500r/min for 15 min. The optical densities (OD) of the extracted acetone at 630, 647, 664 and 750 nm were measured through a Ultrospec 3000 spectrophotometer (Pharmacia Biotech., England) in 1-cm quartz cuvettes. The concentration of chlorophyll-*a* can be obtained by the following equation:

$$\text{chlorophyll } a = \frac{[11.85(A_3 - A_4) - 1.54(A_2 - A_4) - 0.08(A_1 - A_4)]V_1}{V_2 L} \tag{3}$$

where A_1, A_2, A_3, A_4 represent the absorbance at wavelength 630 nm, 647 nm, 664 nm and 750 nm, respectively. V_1 is the volume of 90% acetone. V_2 is the volume of filtered samples, in this paper, 20 mL of the treated algae samples are filtered by low vacuum. L is the optical path of quartz cuvettes (1 cm).

Therefore, the cell disruption efficiency of cavitation treatment can be quantified according to the concentration variation of the algae

suspensions:

$$D(\%) = \left(\frac{Cha_0 - Cha_T}{Cha_0}\right) \times 100 \quad (4)$$

where Cha is the chlorophyll-*a* concentration of cell suspensions, subscript *0* and *T* are the samples before and after treatment.

3. Results and discussions

3.1. The removal of M. aeruginosa by JPCR

3.1.1. The inhibitory effect on the photosynthetic activity of M. aeruginosa

The photosynthetic activity of *M. aeruginosa* can be influenced by the cavitation treatment in JPCR, thus contributing to the removal of *M. aeruginosa.* In this paper, maximal PSII quantum yield Y and maximal relative electron transport rates ETR_{max} are used to evaluate the photosynthetic activity of algae cells treated by JPCR.

Fig. 3 shows the changes in Y and ETR_{max} after treated by JPCR for different hours (p_{in} = 700 kPa, h = 0.087). The control samples were treated at the non-cavitation stage, in which the JPCR was adjusted to the non-cavitation state and the control samples were circulated by the centrifugal pump without cavitation. The results show that the values of Y and ETR_{max} gradually decrease during the cavitation treatment in JPCR, while the values of Y and ETR_{max} of the control samples remain almost constant, indicating that an important portion of the PSII reaction center is damaged by JPCR, and thus leading to the reduction of the electron transport chain. The result of control samples also shows that the centrifugal pump has little effect on *M. aeruginosa.* The photosynthetic activity of algae cells after treated by JPCR decreases sharply, which also affects the growth and reproduction of algae cells. This is mainly contributed to the cavitation effects generated during the cavitation collapse in JPCR [47]. Extremely high temperatures (10000 K), high-pressure pulse (1000 atm), microjet, shear force and highly reactive hydroxyl radicals formed during the collapse of cavitation bubbles greatly damage the photosynthetic apparatus [8,47,48]. Thus, the photosynthetic activity of *M. aeruginosa* is inhibited after cavitation treatment in JPCR. The chloroplast is the most important photosynthetic organ in *M. aeruginosa* cells. The thylakoids in *M. aeruginosa* cells are flattened vesicles on the long axis of the chloroplast, on which the light reaction is carried out. During the cavitation treatment, the thylakoids in the chloroplast are easily damaged [48], which seriously hinders photochemical reaction in the PSII reaction center and leads to the decrease of photosynthetic activity [48].

3.1.2. The inhibitory effect on the growth of M. aeruginosa

The decrease of photosynthetic activity would hinder the growth of *M. aeruginosa*, which also contributes to the algal removal. The growth of *M. aeruginosa* is evaluated by the optical density (OD_{680}) immediately after cavitation treatment and grown continuously in the incubator for 3 days.

Fig. 4 shows the change in optical density (OD_{680}) of algae cells suspension (a) immediately after treated by JPCR for different hours and (b) during 3 days culture after treated by JPCR for different hours, respectively (p_{in} = 700 kPa, h = 0.087). Fig. 4 (a) shows that the optical density of algal cells decreases significantly after treated by JPCR for 6 h, indicating that the structure of algal cells is immediately destroyed after the cavitation treatment, and the intracellular pigments are released outside the cells and gradually decomposed, resulting in the loss of cellular activity and a decrease in the total biomass of algal cells.

Fig. 4 (b) shows that the optical density of the control samples repeatedly decreases and increases under the dark-light cycle, but the overall trend of the optical density is increasing over 3 days. We also observed that most of the algal cells did not coagulate and settle to the bottom over 3 days culture, indicating that the algal cells without treatment in JPCR are biologically active. The algal cells can still absorb light and carbon dioxide, thus maintaining biologically active. However, the optical density of algae cell suspension after treatment for different hours shows a steady decreasing trend over 3 days, and finally decreases to the lowest value and remains stable. The coagulation of algae cells is observed in all treated samples and finally settle to the bottom. Meanwhile, the longer the treatment time, the faster the optical density of the treated cells suspension decreases to the lowest value. However, the optical density could not be reduced to zero. This can be contributed to the impurities in the samples, as the algal samples are collected from the field, but it does not mean that the treated samples with the lowest optical density still maintain biologically active.

The inhibitory effect on algal growth may be related to the mechanical damage of the gas vesicles and photosynthetic apparatus caused by cavitation [49]. The algal cells lose the ability to float when the gas vesicles are damaged, thus leading to the sinking of algal cells. Therefore, the cells lose their stability and settle down at the bottom [50]. Finally, the algal cells settled at the bottom cannot fully absorb sunlight and carbon dioxide, and gradually die in the absence of nutrients and sunlight.

3.1.3. Cell disruption of M. aeruginosa in JPCR

Cavitation bubbles collapse greatly damages cell structures and rupture the cell membrane, resulting in the release of extracellular organic matter. In this paper, the concentration of chlorophyll-*a* could be used to quantify the cell disruption efficiency.

Fig. 5 shows the changes in (a) chlorophyll-*a* concentration of the extracted cell suspensions and (b) the corresponding cell disruption efficiency after treated by JPCR for different hours (p_{in} = 700 kPa, h = 0.087). The chlorophyll-*a* concentration of the treated samples shows a steady decreasing trend, while the chlorophyll-*a* concentration of the control samples remains constant. The cell disruption efficiency reaches 17.4% after 6 h treatment in JPCR.

To demonstrate the damage on algal cells by cavitation treatment in

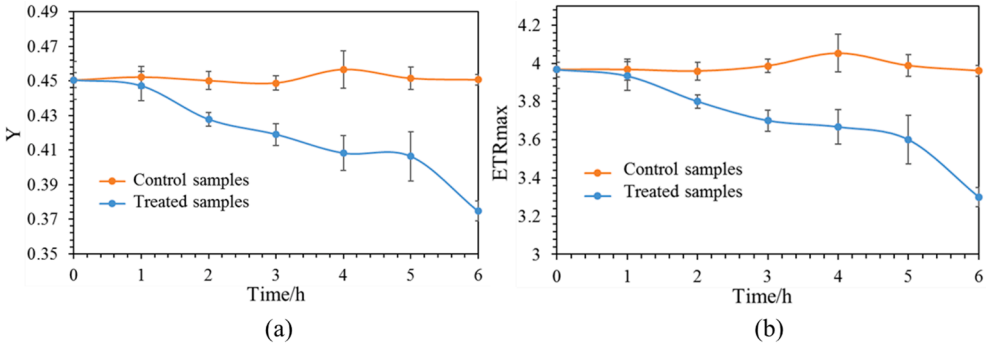

Fig. 3. The change in (a) maximal PSII quantum yield (Y) and (b) maximal relative electron transport rates (ETR_{max}) of the cell suspension after treated by JPCR (p_{in} = 700 kPa, h = 0.087).

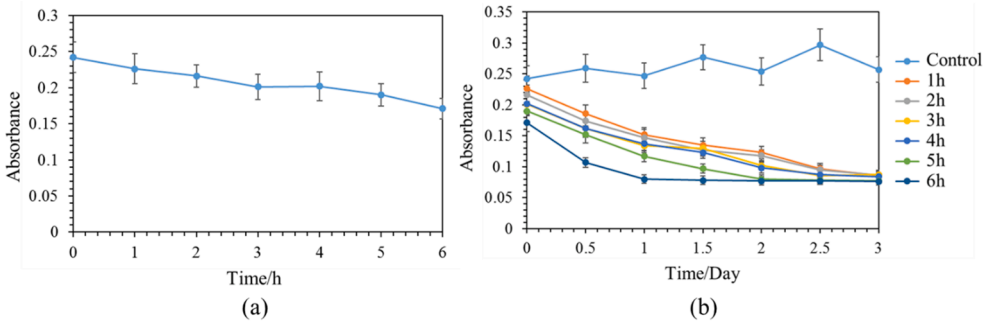

Fig. 4. The variation of optical density (a) immediately after treated by JPCR for different hours and (b) during 3 days culture (p_{in} = 700 kPa, h = 0.087).

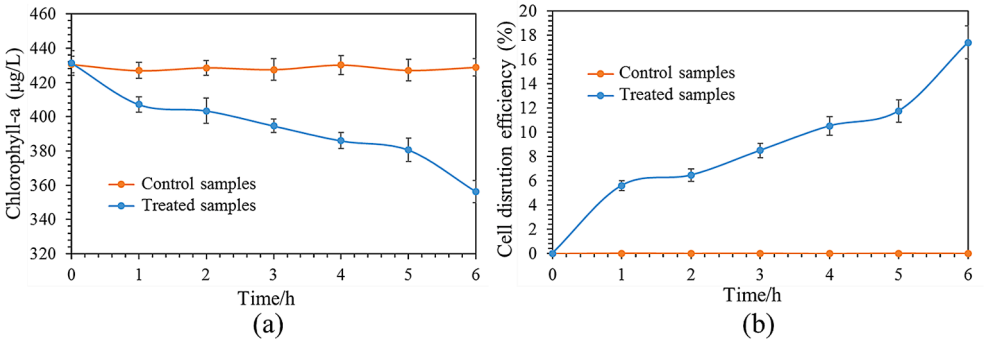

Fig. 5. The change in (a) chlorophyll-*a* concentration and (b) the corresponding cell disruption efficiency after treated by JPCR for different hours (p_{in} = 700 kPa, h = 0.087).

JPCR, fluorescence microscope and scanning electron microscope (SEM) are used to detect changes in cell membrane permeability and cell morphology after cavitation treatment. When the algal cells are treated by JPCR, the intracellular apparatus are greatly inhibited and damaged, leading to the loss of metabolic (esterase) activity and changes in cell membrane permeability. The treated algal samples are examined with an FDA reagent, and intact cells fluoresce green fluorescence when they are observed by fluorescence microscope at wavelength 493 nm, while almost dead cells do not fluoresce green due to the loss of metabolic (esterase) activity and changes in cell membrane permeability [8,51–53]. Fig. 6 shows the fluorescence microscope image of treated and untreated algal cells stained by the FDA reagent. The results show that the untreated algal cells fluoresce green fluorescence, which could not be observed in the treated algal cells, suggesting that metabolic (esterase) activity is greatly influenced by JPCR.

The cell morphology of untreated and treated algal cells observed by SEM is shown in Fig. 7. Fig. 7 (a) shows the intact cell structure of untreated algal cells, which are spherical with viscous material attached to the cell surface. However, after 6 h treatment, all cells are no longer spherical and clear depressions on the cells could be observed, even some cells show obvious rupture with the loss of intracellular material.

Fig. 8 shows the schematic overview of possible cell disruption mechanisms in JPCR. The possible cell disruption mechanism of JPCR could be contributed to the synergy of mechanical effect, thermal effect and chemical effect generated during the collapse of cavitation bubbles [11,54]. The mechanical effect mainly includes the high shear stresses, shock wave, and microjet generated during the development and collapse of cavitation bubbles. High shear stresses are formed in JPCR between the driving flow and the suction flow owing to the velocity gradient between these two flows. The high shear stresses can be as high as 3.5 kPa [55]. Shock waves are induced by adiabatic compression of bubbles during rapid changes when the cavitation bubbles collapse violently in the diffuser, with propagating speed up to almost 4000 m/s [56] and the pressures as high as 6000 or 7150 MPa [56,57]. The violent shape change of bubbles induces a high-speed microjet with a maximum speed over 150 m/s [58]. These mechanical effects weaken or tear the outer layer of *M. aeruginosa* cells, resulting in obvious rupture and the loss of intracellular material. Hot spots induced during the bubbles

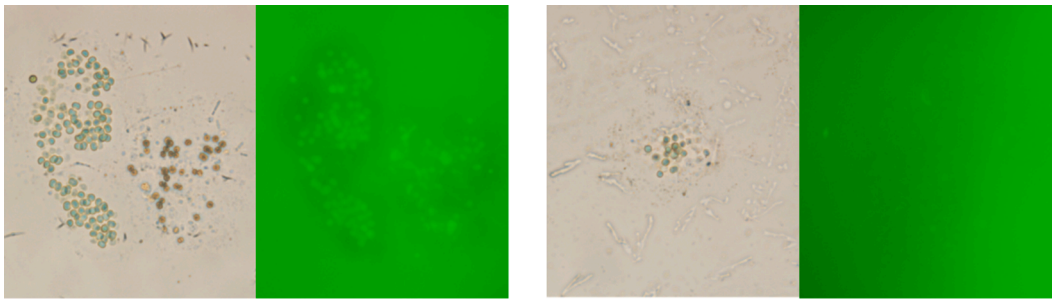

(a) Untreated algal cells (b) Treated algal cells

Fig. 6. Fluorescence microscope image of (a) untreated algal cells and (b) treated algal cells.

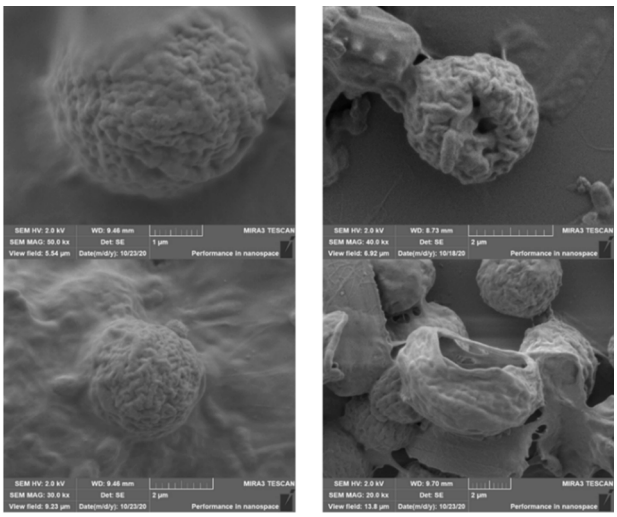

Fig. 7. Stereoscan electron micrographs of (a) untreated algal cells and (b) treated algal cells.

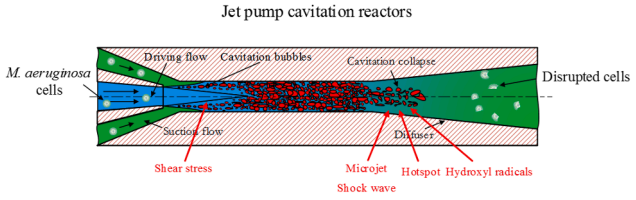

Fig. 8. Possible cell disruption mechanism of JPCR.

collapse can reach as high as 50000 K [59], which could affect the integrity of the outer layer of algal cells and make them more susceptible to the damage of the mechanical effects. Moreover, highly reactive hydroxyl radicals (OH·) [60] generated by the sonolysis of water molecules can oxidize sulfhydryl groups and double bonds on the surface of proteins, lipids and membranes [61,62], resulting in the change of cell membrane permeability.

3.2. Influence of flow conditions on cell disruption efficiency

The optimization of flow condition for JPCR is of great importance to get the maximum algal removal effect. In this section, the cell disruption efficiency is used as an intuitive index for optimizing the flow conditions.

3.2.1. The effect of inlet pressure on cell disruption efficiency

Higher inlet pressures increase turbulence levels and local pressure oscillations, thus enhancing the cavitation effects [46]. However, at very high inlet pressures supercavitation could be formed and cavitation bubbles coalesce with each other, resulting in a progressive decrease of cavitation effects [17]. Therefore, there seems to be a critical inlet pressure where maximum algae removal effect can be achieved. In this paper, algal cell suspensions are treated at different inlet pressures to investigate the effect of inlet pressure on algal cell disruption efficiency in JPCR.

The cell disruption efficiencies after JPCR treatment at different inlet pressure are illustrated in Fig. 9. With the increasing inlet pressure, the cell disruption efficiency shows an increasing trend, but no critical inlet pressure is observed. When the inlet pressure is higher than 300 kPa, cavitation occurs in JPCR and the algal cell disruption is detected in the treated algal suspensions, and the highest cell disruption efficiency

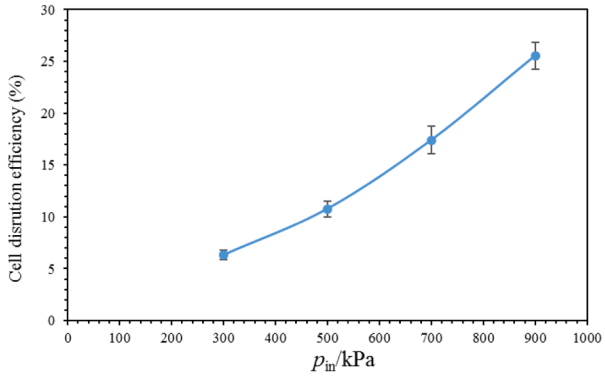

Fig. 9. The variation of cell disruption efficiency at different inlet pressures.

(25.54%) is observed at inlet pressure 900 kPa.

The cavitation mechanisms and the structure of the throat and diffuser are the main reasons why the critical inlet pressure could not be observed in JPCR. The high-speed driving flow entrains the suction flow into the suction chamber, and cavitation occurs easily in the shear layer between these two flows. The combination of low local pressure and shear flow results in more intensive cavitation at higher inlet pressure. A low-pressure zone is also formed in the throat, which greatly promotes cavitation in JPCR. The developed cavitation cloud collapses violently in the divergent diffuser without bubbles coalescing with each other. So both fully developed cavitation cloud and sufficient cavitation collapse intensity could be guaranteed in JPCR even at high inlet pressure. Therefore, the cell disruption efficiency increases with the increasing inlet pressure with no inflection point.

3.2.2. The effect of outlet pressure on cell disruption efficiency

The pressure ratio increases as the outlet pressure increases at constant inlet pressure, resulting in different cavitation performances [29,43]. Fig. 10 and Fig. 11 show the fundamental performance curve of JPCR and the development of cavitation cloud at typical cavitation stages marked (1)-(5). With the increase of outlet pressure [29], the development of cavitation cloud in JPCR could be divided into four stages: the inception and developing cavitation stage, unstable limited operation cavitation stage, stable limited operation cavitation stage, and a special operating condition called the reverse flow cavitation stage, where the driving flow sprays into the throat but flow back into the suction chamber. In the inception and developing cavitation stage (Fig. 11(2)), the cavitation gradually appears at the interface of the driving flow and suction flow and then develops in the throat. In this stage, the intensity of cavitation development and collapse is so weak

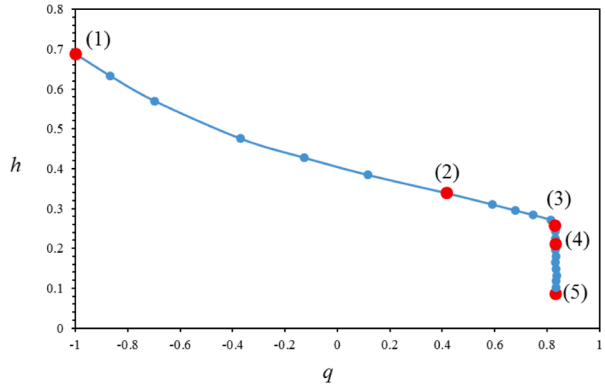

Fig. 10. The fundamental performance curve of JPCR (p_{in} = 700 kPa) and the typical cavitation stage marked (1)-(5).

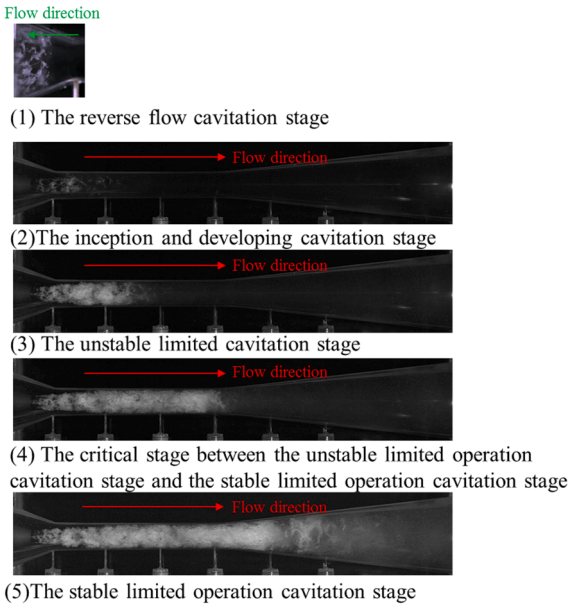

Fig. 11. The instantaneous image of the typical cavitation stage (1)-(5) (p_{in} = 700 kPa).

that the algal removal experiments are not conducted in this stage. In the unstable limited operation cavitation stage (Fig. 11(3)), the flow ratio reaches its limit and the cavitation cloud oscillates in the throat. In the stable limited operation cavitation stage (Fig. 11(5)), cavitation clouds are fully developed and the clusters of cavitation cloud shed and collapse in the diffuser. When the flow ratio reaches the limit, the cavitation cloud fully develops and collapses violently, so the critical stage (Fig. 11 (4)) between the unstable limited operation stage and stable limited operation cavitation is also chosen as the operation condition for algal removal experiments. In this stage, the fully developed cavitation cloud collapses at the throat exit instantly due to the high backpressure. The reverse cavitation flow stage (Fig. 11(1)) is also chosen because of the high potential for cell disruption due to the high-pressure pulsation in this cavitation stage [44].

Fig. 12 shows the cell disruption efficiency variation at different cavitation stages. The results show that satisfactory cell disruption efficiency can be obtained under the stable limited operation cavitation stage, critical stage and reverse cavitation flow condition. However, the cell disruption efficiency is much lower at the unstable limited operation cavitation stage. The results also show that the highest cell disruption efficiency (25.05%) is achieved at the critical cavitation stage, and the cell disruption efficiency is higher than that at the stable limited operation cavitation stage and the reverse cavitation flow stage. As the outlet pressure increases, the stable limited operation cavitation stage transfers to the critical stage, and the cavitation cloud shrinks into the throat. At high backpressure, the cavitation cloud collapses violently at the throat exit, generating high-pressure pulsation and leading to the highest cell disruption efficiency at this critical cavitation stage., Though cavitation cloud is fully developed and intensive cavitation cloud is generated in the stable limited operation cavitation stage (5), the cavitation bubbles coalesce with each other, resulting in a progressive decrease of cavitation effects and a lower cell disruption efficiency than that in the critical cavitation stage (4).

4. Conclusions

Algal blooms are serious problems in eutrophic water bodies and jet pump cavitation reactor (JPCR) has shown great potential for water treatment with high cavitation intensity. In this paper, a jet pump cavitation reactor (JPCR) is developed for the removal of *Microcystis*

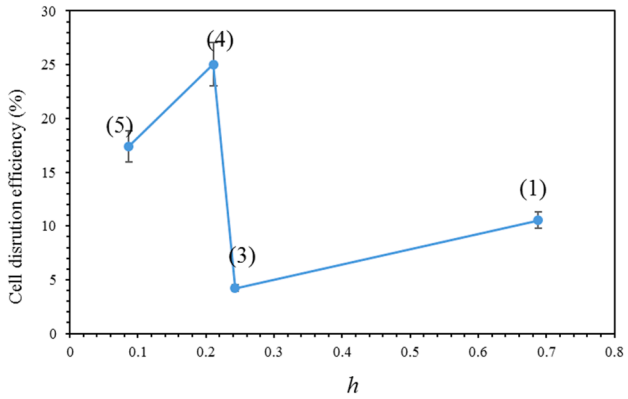

Fig. 12. The variation of cell disruption efficiency at different pressure ratios.

aeruginosa in a pilot-scale. After treated by JPCR, the maximal PSII quantum yield Y, maximal relative electron transport rates ETR_{max} and the optical density of algal cell suspensions decrease, indicating JPCR greatly inhibits the photosynthetic activity and growth of algal cells. Based on the variation of chlorophyll-*a* concentration, a high cell disruption efficiency could be detected in treated algal cells. Significant changes in cell membrane permeability and rupture of cell structure could be observed by fluorescence microscope and scanning electron microscope (SEM). The possible cell disruption mechanism of JPCR could be contributed to the synergy of mechanical effects, thermal effects and chemical effects generated during the collapse of cavitation bubbles. Then the optimization of operating conditions in JPCR is also investigated, and results show that the algal cell disruption efficiency is improved at higher inlet pressure and the cavitation stage between the unstable limited operation cavitation stage and stable limited operation cavitation stage.

JPCR could be applied not only in the fields of algal blooms control but also in the field of biomass production, biofuels production, ballast water treatment, water disinfection, etc, where cell disruption is needed. Further researches on the cell disruption mechanism, structural optimization, and scale-up are needed in the future.

CRediT authorship contribution statement

Shuangjie Xu: Conceptualization, Methodology, Formal analysis, Investigation, Writing – original draft, Writing – review & editing, Visualization. **Jiong Wang:** Investigation, Methodology. **Wei Chen:** Supervision. **Bin Ji:** Supervision. **Hengfei Yan:** Supervision. **Zuti Zhang:** Funding acquisition, Supervision. **Xinping Long:** Investigation, Writing – review & editing, Funding acquisition.

Declaration of Competing Interest

The authors declare that they have no known competing financial interests or personal relationships that could have appeared to influence the work reported in this paper.

Acknowledgments

This work was financially supported by the National Natural Science Foundation of China (Project Nos. 12072243, 512072243, 51679169, and 11472197).

References

[1] W. Lei, Q. Junlian, H. Yinghui, Pre-oxidation with KMnO4 changes extra-cellular organic matter's secretion characteristics to improve algal removal by coagulation with a low dosage of polyaluminium chloride, J. Environ. Sci. (2013).
[2] X. Jin, Q. Xu, C. Huang, Current status and future tendency of lake eutrophication in China, Sci. China 48 (Suppl 2) (2005) 948.

[3] V. Klemas, Remote sensing of algal blooms: an overview with case studies, J. Coastal Res. 28 (2012) 34–43.
[4] V. Vasconcelos, E. Pereira, Cyanobacteria diversity and toxicity in a wastewater treatment plant (Portugal), Water Res. 35 (2001) 1354–1357.
[5] X. Zhang, C. Chen, J. Ding, A. Hou, Y. Li, Z. Niu, X. Su, Y. Xu, E.A. Laws, The 2007 water crisis in Wuxi, China: Analysis of the origin, J. Hazard. Mater. 182 (2010) (2007) 130–135.
[6] G. Mancuso, G.F. Bencresciuto, S. Lavrnić, A. Toscano, Diffuse Water Pollution from Agriculture: A Review of Nature-Based Solutions for Nitrogen Removal and Recovery, Water 13 (2021) 1893.
[7] J. Ma, W. Liu, Effectiveness and mechanism of potassium ferrate (VI) preoxidation for algae removal by coagulation, Water Res. 36 (2002) 871–878.
[8] D. Jančula, P. Mikula, B. Maršálek, P. Rudolf, F. Pochylý, Selective method for cyanobacterial bloom removal: hydraulic jet cavitation experience, Aquacult. Int. 22 (2014) 509–521.
[9] Z. Wu, H. Shen, B. Ondruschka, Y. Zhang, W. Wang, D.H. Bremner, Removal of blue-green algae using the hybrid method of hydrodynamic cavitation and ozonation, J Hazard Mater 235–236 (2012) 152–158.
[10] G. Zhang, P. Zhang, M. Fan, Ultrasound-enhanced coagulation for Microcystis aeruginosa removal, Ultrason. Sonochem. 16 (2009) 334–338.
[11] M. Zupanc, Z. Pandur, T. Stepisnik Perdih, D. Stopar, M. Petkovsek, M. Dular, Effects of cavitation on different microorganisms: The current understanding of the mechanisms taking place behind the phenomenon. A review and proposals for further research 57 (2019) 147–165.
[12] Franc, P. Jean, Fundamentals of Cavitation, 2005.
[13] K. Masaki, M. Patrick, X. King, E. Wu, M. Joyce, Effect of sonication frequency on the disruption of algae, Ultrason. Sonochem. 31 (2016) 157–162.
[14] S. Pathania, Q.T. Ho, S.A. Hogan, N. Mccarthy, J.T. Tobin, Applications of hydrodynamic cavitation for instant rehydration of high protein milk powders, 225 (2018) 18–25.
[15] D. Kim, E.K. Kim, H.G. Koh, K. Kim, J.I. Han, K.C. Yong, Selective removal of rotifers in microalgae cultivation using hydrodynamic cavitation, 28 (2017) 24-29.
[16] C. Yi, Q. Lu, Y. Wang, Y. Wang, B. Yang, Degradation of organic wastewater by hydrodynamic cavitation combined with acoustic cavitation, 43 (2018) 156-165.
[17] G. Mancuso, M. Langone, G. Andreottola, A critical review of the current technologies in wastewater treatment plants by using hydrodynamic cavitation process: principles and applications, J. Environ. Health Sci. Eng. 18 (2020).
[18] G. Mancuso, M. Langone, R. Di Maggio, A. Toscano, G. Andreottola, Effect of hydrodynamic cavitation on flocs structure in sewage sludge to increase stabilization for efficient and safe reuse in agriculture, Biorem. J. 26 (1) (2022) 41–52.
[19] G. Mancuso, M. Langone, M. Laezza, G. Andreottola, Decolourization of Rhodamine B: A swirling jet-induced cavitation combined with NaOCl, Ultrason. Sonochem. 32 (2016) 18–30.
[20] G. Mancuso, M. Langone, G. Andreottola, L. Bruni, Effects of hydrodynamic cavitation, low-level thermal and low-level alkaline pre-treatments on sludge solubilisation, Ultrason. Sonochem. 59 (2019) 104750-.
[21] G. Mancuso, M. Langone, G. Andreottola, A swirling jet-induced cavitation to increase activated sludge solubilisation and aerobic sludge biodegradability, Ultrason. Sonochem. 35 (2017) 489–501.
[22] G. Zhang, P. Zhang, H. Liu, B.o. Wang, Ultrasonic damages on cyanobacterial photosynthesis, Ultrason. Sonochem. 13 (6) (2006) 501–505.
[23] J.A. Gerde, M. Montalbo-Lomboy, L. Yao, D. Grewell, T. Wang, Evaluation of microalgae cell disruption by ultrasonic treatment, Bioresour. Technol. 125 (2012) 175–181.
[24] M.H. Dehghani, Removal of cyanobacterial and algal cells from water by ultrasonic waves — A review, J. Mol. Liq. 222 (2016) 1109–1114.
[25] K.K. Jyoti, A.B. Pandit, Water disinfection by acoustic and hydrodynamic cavitation, Biochem. Eng. J. 7 (3) (2001) 201–212.
[26] S. Xu, J. Wang, H. Cheng, B. Ji, X. Long, Experimental Study of the Cavitation Noise and Vibration Induced by the Choked Flow in a Venturi Reactor, Ultrason. Sonochem. 67 (2020), 105183.
[27] H.K. Suh, C.S. Lee, Effect of cavitation in nozzle orifice on the diesel fuel atomization characteristics, Int. J. Heat Fluid Flow 29 (2008) 1001–1009.
[28] Q. Wu, B. Huang, G. Wang, Y. Gao, Experimental and numerical investigation of hydroelastic response of a flexible hydrofoil in cavitating flow, Int. J. Multiph. Flow 74 (2015) 19–33.
[29] X. Long, H. Yao, J. Zhao, Investigation on mechanism of critical cavitating flow in liquid jet pumps under operating limits, Int. J. Heat Mass Transf. 52 (2009) 2415–2420.
[30] H. Chen, L. Jiang, D. Chen, J. Wang, Damages on steel surface at the incubation stage of the vibration cavitation erosion in water, Wear 266 (2008) 69–75.
[31] E. Hutli, M.S. Nedeljkovic, N.A. Radovic, A. Bonyár, The relation between the high speed submerged cavitating jet behaviour and the cavitation erosion process, Int. J. Multiph. Flow 83 (2016) 27–38.
[32] C. Park, H. Seol, K. Kim, W. Seong, A study on propeller noise source localization in a cavitation tunnel, Ocean Eng. 36 (2009) 754–762.
[33] X. Sun, J. Liu, L.i. Ji, G. Wang, S. Zhao, J.Y. Yoon, S. Chen, A review on hydrodynamic cavitation disinfection: The current state of knowledge, Sci. Total Environ. 737 (2020) 139606, https://doi.org/10.1016/j.scitotenv.2020.139606.
[34] G. Mancuso, Experimental and numerical investigation on performance of a swirling jet reactor, Ultrason. Sonochem. 49 (2018) 241–248.
[35] M. Schlender, A. Spengler, H.P. Schuchmann, High-pressure emulsion formation in cylindrical coaxial orifices: Influence of cavitation induced pattern on oil drop size, Int. J. Multiph. Flow 74 (2015) 84–95.
[36] J. Zhu, H. Xie, K. Feng, X. Zhang, M. Si, Unsteady cavitation characteristics of liquid nitrogen flows through venturi tube, Int. J. Heat Mass Transf. 112 (2017) 544–552.
[37] D. Bertoldi, C.C. Dallalba, J.R. Barbosa Jr, Experimental investigation of two-phase flashing flows of a binary mixture of infinite relative volatility in a Venturi tube, Exp. Therm. Fluid Sci. 64 (2015) 152–163.
[38] K. Ariafar, D. Buttsworth, G. Al-Doori, R. Malpress, Effect of mixing on the performance of wet steam ejectors, Energy 93 (2015) 2030–2041.
[39] H. Lu, Theory and application of injection technolog, 2004.
[40] X. Lu, D. Wang, W. Shen, C. Zhu, G. Qi, Experimental investigation on liquid absorption of jet pump under operating limits, Vacuum 114 (2015) 33–40.
[41] M. Xu, B. Ji, J. Zou, X. Long, Experimental investigation on the transport of different fish species in a jet fish pump, Aquacult. Eng. 79 (2017) 42–48.
[42] S. Sherif, W. Lear, J. Steadham, P. Hunt, J. Holladay, Analysis and modeling of a two-phase jet pump of a thermal management system for aerospace applications, Int. J. Mech. Sci. 42 (2000) 185–198.
[43] X. Long, J. Zhang, Q. Wang, L. Xiao, M. Xu, Q. Lyu, B. Ji, Experimental investigation on the performance of jet pump cavitation reactor at different area ratios, Exp. Therm. Fluid Sci. 78 (2016) 309–321.
[44] X. Long, J. Wang, J. Zhang, B. Ji, Experimental investigation of the cavitation characteristics of jet pump cavitation reactors with special emphasis on negative flow ratios, Exp. Therm Fluid Sci. 96 (2018) 33–42.
[45] J. Wang, S. Xu, H. Cheng, B. Ji, J. Zhang, X. Long, Experimental investigation of cavity length pulsation characteristics of jet pumps during limited operation stage, Energy 163 (2018) 61–73.
[46] J. Wang, H. Cheng, S. Xu, B. Ji, X. Long, Performance of cavitation flow and its induced noise of different jet pump cavitation reactors, Ultrason. Sonochem. 55 (2019) 322–331.
[47] P.R. Gogate, G.S. Bhosale, Comparison of effectiveness of acoustic and hydrodynamic cavitation in combined treatment schemes for degradation of dye wastewaters, Chem. Eng. Process. Process Intensif. 71 (2013) 59–69.
[48] Y. Xu, J. Yang, Y. Wang, F. Liu, J. Jia, The effects of jet cavitation on the growth of Microcystis aeruginosa, J. Environ. Sci. Health, Part A 41 (2006) 2345–2358.
[49] R. Henderson, S. Parsons, B. Jefferson, Successful removal of algae through the control of zeta potential, Sep. Sci. Technol. 43 (2008) 1653–1666.
[50] P. Li, Y. Song, S. Yu, H.-D. Park, The effect of hydrodynamic cavitation on Microcystis aeruginosa: Physical and chemical factors, Chemosphere (2015).
[51] R.H. Regel, J.M. Ferris, G.G. Ganf, J.D. Brookes, Algal esterase activity as a biomeasure of environmental degradation in a freshwater creek, Aquat. Toxicol. 59 (2002) 209–223.
[52] T. Amano, K.I. Hirasawa, M. O'Donohue, J.C. Pernolle, Y. Shioi, A versatile assay for the accurate, time-resolved determination of cellular viability, Anal. Biochem. 314 (2003) 1–7.
[53] L.B. Chen, W.Y. Liang, J.H. Qu, M.S. Xie, H.J. Liu, The viability determination of cyanobacteria by double staining with fluorescein diacetate and propidium iodide, Environ. Chem. 24 (2005) 554–557.
[54] M. Dular, T. Griessler-Bulc, I. Gutierrez-Aguirre, E. Heath, T. Kosjek, A. Krivograd Klemenčič, M. Oder, M. Petkovšek, N. Rački, M. Ravnikar, A. Šarc, B. Širok, M. Zupanc, M. Žitnik, B. Kompare, Use of hydrodynamic cavitation in (waste)water treatment, Ultrason. Sonochem. 29 (2016) 577–588.
[55] R. Dijkink, C.D. Ohl, Measurement of cavitation induced wall shear stress, Appl. Phys. Lett. 93 (2008) 58.
[56] R. Pecha, B. Gompf, Microimplosions: cavitation collapse and shock wave emission on a nanosecond time scale, Phys. Rev. Lett. 84 (2000) 1328.
[57] A. Vogel, S. Busch, U. Parlitz, Shock wave emission and cavitation bubble generation by picosecond and nanosecond optical breakdown in water, The Journal of the Acoustical Society of America 100 (1996) 148–165.
[58] A. Vogel, W. Lauterborn, R. Timm, Optical and acoustic investigations of the dynamics of laser-produced cavitation bubbles near a solid boundary, J. Fluid Mech. 206 (1989) 299–338.
[59] K.S. Suslick, D.A. Hammerton, R.E. Cline, Sonochemical hot spot, J. Am. Chem. Soc. 108 (1986) 5641–5642.
[60] G. Boczkaj, A. Fernandes, Wastewater treatment by means of advanced oxidation processes at basic pH conditions: a review, Chem. Eng. J. 320 (2017) 608–633.
[61] M. Drabkova, H.C.P. Matthijs, W. Admiraal, B. Marsalek, Selective effects of H2O2 on cyanobacterial photosynthesis, Photosynthetica 45 (2007) 363–369.
[62] G. McDonnell, A.D. Russell, Antiseptics and disinfectants: activity, action, and resistance, Clin. Microbiol. Rev. 12 (1999) 147–179.